Porphyrinoids

Deutsche Ausgabe: DOI: 10.1002/ange.201602083
Internationale Ausgabe: DOI: 10.1002/anie.201602083

Aromaticity Reversal in the Lowest Excited Triplet State of Archetypical Möbius Heteroannulenic Systems

Juwon Oh, Young Mo Sung, Woojae Kim, Shigeki Mori, Atsuhiro Osuka, and Dongho Kim**

Abstract: *The aromaticity reversal in the lowest triplet state (T_1) of a comparable set of Hückel/Möbius aromatic metalated expanded porphyrins was explored by optical spectroscopy and quantum calculations. In the absorption spectra, the T_1 states of the Möbius aromatic species showed broad, weak, and ill-defined spectral features with small extinction coefficients, which is in line with typical antiaromatic expanded porphyrins. In combination with quantum calculations, these results indicate that the Möbius aromatic nature of the S_0 state is reversed to Möbius antiaromaticity in the T_1 state. This is the first experimental observation of aromaticity reversal in the T_1 state of Möbius aromatic molecules.*

The concept of aromaticity, the most fundamental and widely studied subject in physical organic chemistry, has been frequently utilized to gauge the chemical properties of molecular systems.[1,2] Conventionally, the aromatic nature of π-conjugated cyclic compounds is assigned according to the Hückel rule, which dictates planar annulenes with $(4n+2)\pi$ and $(4n)\pi$ electrons to be aromatic and antiaromatic, respectively. In 1964, Heilbronner proposed this counting rule to be reversed in twisted annulenes bearing Möbius topology.[3] The realization of Möbius aromatic molecules has to overcome difficulties associated with the large ring strains arising from Möbius geometry and the maintenance of the overall macrocyclic conjugation.[4] Despite these difficulties, the first Möbius aromatic molecule was synthesized on the basis of a paper model strategy by Herges et al.[5] Subsequently, Latos-Grażyński et al. reported solvent- and temperature-dependent absorption changes for *p*-benzi-[28]hexaphyrin, which has been explained in terms of conformational changes involving a Möbius aromatic expanded hexaphyrin.[6] Independently, our group demonstrated that meso-aryl expanded porphyrins are suitable platforms to realize Möbius aromatic and antiaromatic systems with distinct diatropic and paratropic ring currents, respectively.[7]

The π-electron counting rule is also reversely applied to annulenes in the T_1 state. In 1972, Baird proposed that the aromaticity in the T_1 excited state should be reversed from that of the S_0 ground state on the basis of the molecular orbital perturbation theory (Baird's rule); that is, a compound with aromaticity (or antiaromaticity) in the S_0 state becomes antiaromatic (or aromatic) in the T_1 state.[8] Inspired by this prediction, there have been numerous attempts to examine Baird's rule by calculating the aromatic stabilization energy (ASE) and nucleus-independent chemical shifts (NICS).[9,10] Furthermore, several experimental observations, where related chemical reactivities have been interpreted by considering the aromatic character of the T_1 states, support the aromaticity reversal in the T_1 state. In an interesting study, Ottosson, Wörner, and co-workers investigated the spectroscopic features of fulvenes and the cyclopentadienyl cation to reveal the lowest excited state aromaticity.[11] In recent years, we have shown that aromaticity reversal occurs both in the T_1 states of Hückel aromatic bis(rhodium(I)) complexes of [26]hexaphyrin and Hückel antiaromatic bis(rhodium(I)) complexes of [28]hexaphyrin and in the S_1 states of internally 1,3-phenylene-bridged Hückel aromatic and antiaromatic [26]- and [28]hexaphyrins by comparing the contrasting spectroscopic features of their excited-state transient absorptions.[12]

Herein, we explored the T_1 state aromaticity of Möbius aromatic expanded porphyrins with the objective to investigate whether Baird's rule is applicable to Möbius aromatic molecules.[9b] Since the monumental reports on the (anti)aromaticity and nonplanar geometry of expanded porphyrins by the groups of Sessler and Vogel,[13] continuous studies have revealed that meso-aryl-substituted expanded porphyrins are sufficiently flexible to accommodate twisted structures of Möbius topology with preservation of the cyclic conjugation, making them suitable for the present study.[7] They can also often adopt both $(4n)\pi$ and $(4n+2)\pi$ electronic states, which may facilitate a comparative analysis of the excited states of Möbius aromatic and antiaromatic congeners possessing similar molecular frameworks.[14] Furthermore, in-depth analyses have demonstrated that the optical properties of expanded porphyrins, including absorption, emission, S_1 lifetime, and nonlinear optical properties, arise from their aromatic and antiaromatic π-electronic nature, providing obvious experimental fingerprints for the determination of the excited-state aromaticity.[15]

In this study, we chose the [28]hexaphyrin Pd^{II} complex Pd28H,[7,16] the N-fused [22]pentaphyrin Rh^{I} complex Rh22P, and the N-fused [24]pentaphyrin Rh^{I} complex Rh24P as our model systems (Figure 1),[17] in which the coordinated metals are expected to promote the intersystem crossing in their S_1

[*] J. Oh, Dr. Y. M. Sung, W. Kim, Prof. Dr. D. Kim
Department of Chemistry
Spectroscopy Laboratory for Functional π-Electronic Systems
Yonsei University, Seoul 120-749 (Korea)
E-mail: dongho@yonsei.ac.kr
Dr. S. Mori, Prof. Dr. A. Osuka
Department of Chemistry, Graduated School of Science
Kyoto University, Kyoto 606-8502 (Japan)
E-mail: osuka@kuchem.kyoto-u.ac.jp

Supporting information for this article can be found under: http://dx.doi.org/10.1002/anie.201602083.

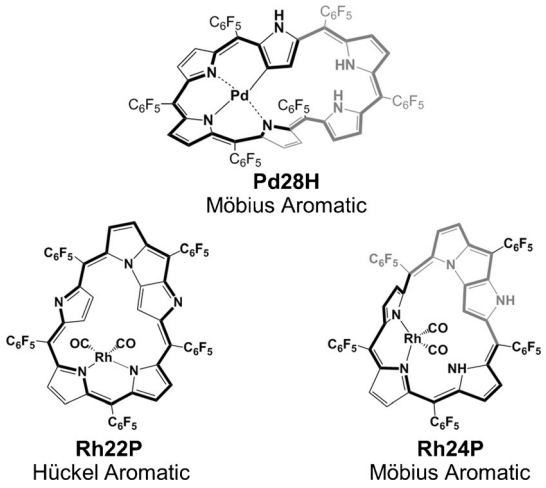

Figure 1. A comparable set of metalated expanded porphyrins: Pd28H, Rh22P, and Rh24P.

states to give the corresponding T_1 states without substantial electronic perturbation. Our previous studies have revealed that Rh22P is a Hückel aromatic molecule and that Pd28H and Rh24P are Möbius aromatic molecules on the basis of their ^{1}H NMR spectra, crystal structures, and theoretical calculations.[16,17] Their ground-state absorption spectra showed features characteristic of aromatic porphyrinoids, intense B bands, and weak but distinct Q-like bands in the visible and near infrared (NIR) regions (Supporting Information, Figure S1), which also indicate that both Möbius and Hückel aromatic expanded porphyrins have similar π-electronic structures despite their different molecular structures.[7,18]

The aromatic nature of Pd28H, Rh22P, and Rh24P was confirmed by their femtosecond time-resolved transient absorption spectra, which all showed strong ground state bleaching (GSB) and relatively weak excited state absorption (ESA) signals (Figures 2 and S2) as characteristic features of aromatic porphyrinoids.[15] These TA spectra of Pd28H, Rh22P, and Rh24P decayed with two time constants on the order of >10 ps and >10 ns, which correspond to the S_1 and T_1 state decays, respectively. These TA spectra indicated that intersystem crossing to the T_1 state was accelerated owing to the heavy-atom effects of the rhodium and palladium ions without significant electronic perturbation and became competitive with the fast decay of the S_1 state (Figure S3).

Global analysis of the TA spectra over the whole 350–1500 nm region by singular value decomposition provided the decay associated spectra (DAS) of the S_1 and T_1 states. As the DAS of the T_1 state should be composed of GSB and ESA signals without stimulated emission (SE) signals, the T_1 absorption spectra of Pd28H, Rh22P, and Rh24P can be obtained by subtraction of the S_0 absorption spectra from the TA spectra (Figure 3).[12] The T_1 state absorption spectrum of Pd28H thus obtained was significantly different from that of the S_0 state, exhibiting broad and weak bands with a tail reaching deep into the NIR region, and its absorbance was greatly reduced (61 000 $cm^{-1}M^{-1}$ at the absorption maximum) compared with that of the S_0 state (147 000 $cm^{-1}M^{-1}$). The

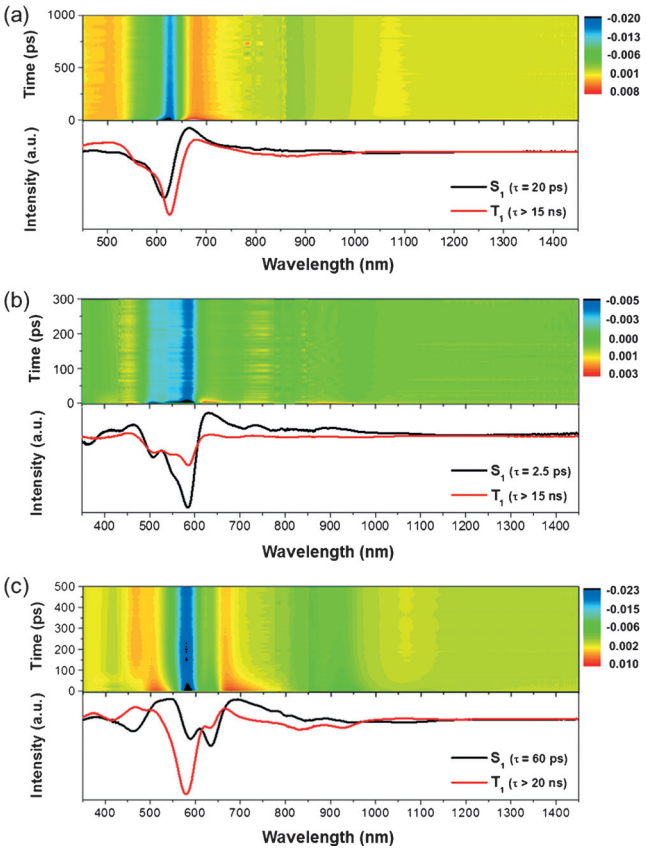

Figure 2. TA contour maps (top) and decay-associated spectra (bottom) of a) Pd28H, b) Rh22P, and c) Rh24P in toluene.

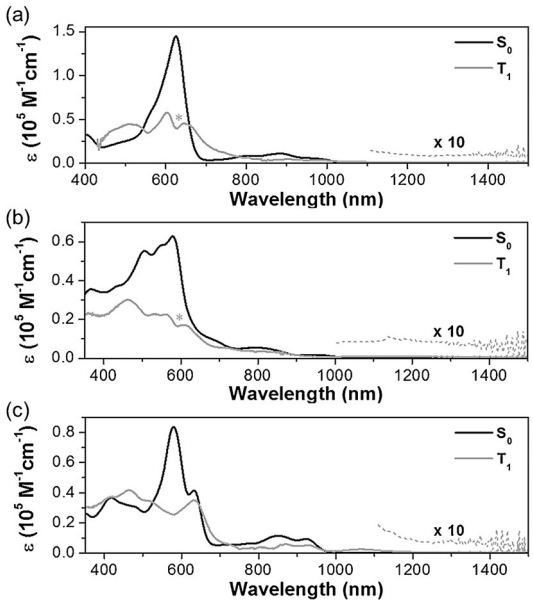

Figure 3. The S_0 and T_1 state absorption spectra of a) Pd28H, b) Rh22P, and c) Rh24P. The asterisks indicate experimental errors that are due to the different spectral resolutions of the two spectrometers used for the ground-state absorption and TA measurements.

observed spectral changes from the S_0 state to the T_1 state of Pd28H are comparable to those of meso-hexakis(trifluoro-

methyl)-substituted [28]hexaphyrins, which can be switched between Möbius aromaticity and Hückel antiaromaticity depending on the temperature.[19] In the respect that Pd28H is a congener of bis(rhodium) complexes of [26]/[28]hexaphyrins (the same molecular framework except for the central metal), its S_0 and T_1 absorption spectra thus resembled those of the bis(rhodium) complexes of aromatic [26]hexaphyrins and antiaromatic [28]hexaphyrins, respectively.[12a] The T_1 state absorption spectra of the N-fused pentaphyrin Rh^I complexes Rh22P and Rh24P exhibited similar broad, weak, and tailing features, and their extinction coefficients were significantly reduced (24000 and 41700 $cm^{-1}M^{-1}$) compared with those of the corresponding S_0 absorption spectra (60800 and 83700 $cm^{-1}M^{-1}$). Collectively, these spectral characteristics of the T_1 states of Pd28H, Rh22P, and Rh24P suggest their antiaromatic nature.

These T_1 absorption spectra enabled us to explore the π-electronic structures of the T_1 states, revealing their (anti)aromaticity. For porphyrinoids, it has been well established that the absorption spectral features reflect their characteristic π-electronic structures, energy-level diagrams, and MO structures;[15] the intense B-like and weak Q-like absorption bands of aromatic porphyrinoids result from the configuration interaction between four degenerate FMOs (HOMO-1, HOMO, LUMO, and LUMO + 1) whereas the broad, weak, and ill-defined absorption bands with characteristic tailing in the NIR region of antiaromatic porphyrinoids are explained in terms of six FMOs (HOMO + 2, HOMO − 1, HOMO, LUMO, LUMO + 1, and LUMO + 2) and forbidden one-photon transitions for HOMO–LUMO and HOMO − 1–LUMO + 1, optically dark state. In the same line, the intense B-like and weak Q-like bands in the visible and NIR regions, respectively, in the S_0 absorption spectra of Pd28H, Rh22P, and Rh24P were explained by the vertical energy transitions between four degenerate FMOs (Figures S4–S7), indicating their aromatic nature with little effects that are due to the coordinated metal.[20] On the other hand, the broad, weak, and tailing features of the T_1 absorption spectra of Pd28H, Rh22P, and Rh24P were well reproduced by the calculated vertical transitions (Figure S4), where the lowest vertical transitions with negligible oscillator strength are well-matched with the characteristics of typical antiaromatic porphyrinoids.[14c] Thus it is likely that the obtained T_1 absorption spectra provide evidence for the antiaromatic character of Pd28H, Rh22P, and Rh24P.

For an in-depth analysis of the aromaticity reversal in the T_1 state, we carried out quantum-chemical calculations for Pd28H, Rh22P, and Rh24P in the S_0 and T_1 states. The NICS values based on the optimized structures clearly illustrated the reversed aromaticity in the T_1 state (Figure S9).[21] Namely, the NICS values at the centers of the macrocycles were estimated to be −9.3, −9.4, and −12.2 ppm for the S_0 states of Pd28H, Rh22P, and Rh24P, respectively, whereas positive NICS values of 10.7–6.6 ppm were calculated for the corresponding T_1 states.

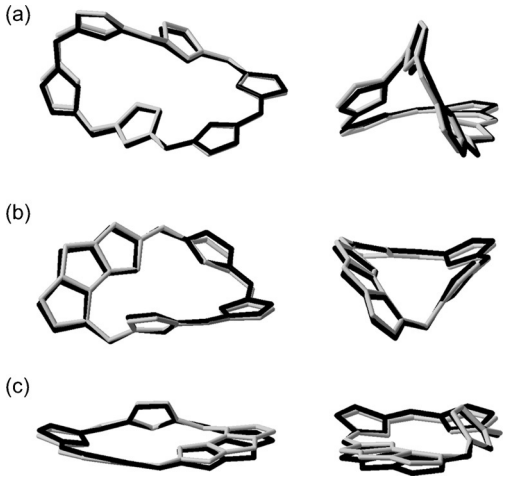

Figure 4. Comparison of the optimized structures of a) Pd28H, b) Rh24P, and c) Rh22P in the S_0 (black) and T_1 (gray) states. Central metal atoms, meso-pentafluorophenyl groups, and hydrogen atoms omitted for clarity.

To probe the structural changes during photoexcitation, the optimized structures for the S_0 and T_1 states of Pd28H, Rh22P, and Rh24P were compared, and an overlay of the S_0 and T_1 structures delineated that their conformations were more twisted in the T_1 states (Figure 4).[9,10] For careful comparison, we measured the dihedral angle distributions, average values, and standard deviations in the S_0 and T_1 states because they provide explicit information on the conformation and cyclic π-conjugation (Table 1 and Figures S10–S12). Compared to the dihedral angles of Pd28H, Rh22P, and Rh24P in the S_0 state, those for the T_1 states were distributed more widely and showed higher averages and standard deviations, which is in agreement with the aromatic character of the S_0 state and the antiaromatic character of the T_1 state. These aspects were also observed in the mean plane deviations (MPD) of Rh22P.[12b] Rh22P showed a smaller MPD in the S_0 state than in the T_1 state (0.401 Å and 0.405 Å, respectively; Figure S13), which supports the aromaticity reversal in the T_1 state. However, in contrast to planar Rh22P, the Möbius twist structures of Pd28H and Rh24P are not suitable for structural analysis with MPD. In this regard, we estimated the linking number (L_k) for Pd28H and Rh24P, which reflects the topological concept of p orbital overlap in the twist conformation.[22] L_k, an integer value corresponding to the number of half-twists in the macrocycle, is composed of the twist (T_w) and writhe (W_r), $L_k = T_w + W_r$. Here, T_w reflects the local torsional twist, and W_r represents the global long-range bending. Whereas the half-twist Möbius aromatic

Table 1: Dihedral angles of Pd28H, Rh22P, and Rh24P in the S_0 and T_1 states.[a]

Dihedral angle	Pd28H		Rh22P		Rh24P	
	S_0	T_1	S_0	T_1	S_0	T_1
range	4.1–46.4°	1.9–59.7°	2.3–32.4°	3.4–40.0°	2.1–50.6°	2.1–61.4°
(Δ)	(42.3°)	(57.8°)	(30.1°)	(36.4°)	(48.5°)	(59.3°)
average	18.0°	19.0°	15.9°	16.9°	21.6°	22.9°
standard deviation	12.9°	16.2°	12.7°	13.0°	15.0°	18.5°

[a] All values correspond to the optimized molecular structures.

compounds Pd28H and Rh24P gave $L_k = 1$ in the S_0 and T_1 states, the values of T_w and W_r were different for the S_0 and T_1 states ($T_w = 0.27/0.30$ and $W_r = 0.73/0.70$ for $Pd28H_{S_0/T_1}$ and $T_w = 0.62/0.65$ and $W_r = 0.38/0.35$ for $Rh24P_{S_0/T_1}$; Table S1). Compared to the T_1 state, the T_w value is smaller in the S_0 state. Given that a small T_w value indicates less local twisting and enhanced conjugation at the expense of smoother bending (larger W_r), the change in the T_w values between the S_0 and T_1 states is in accordance with the reversal of aromaticity and the associated changes in the dihedral angles.[22] Furthermore, the T_w values for Rh24P are even larger than those of Pd28H, which results from larger twisting strain owing to the smaller annulene size and the fused tripentacyclic unit of Rh24P.

Anisotropy of the induced current density (ACID) calculations also support the reversed aromaticity of Pd28H, Rh22P, and Rh24P in the T_1 state.[23] The ACID plots visualize the ring current and direction induced by an applied external magnetic field. Thus clockwise and counterclockwise ring current flows in the ACID plots directly illustrate aromaticity and antiaromaticity, respectively. Pd28H, Rh22P, and Rh24P exhibited contrasting ring current flows between the S_0 and T_1 states (Figures 5 and S14–S16); clockwise ring currents in the

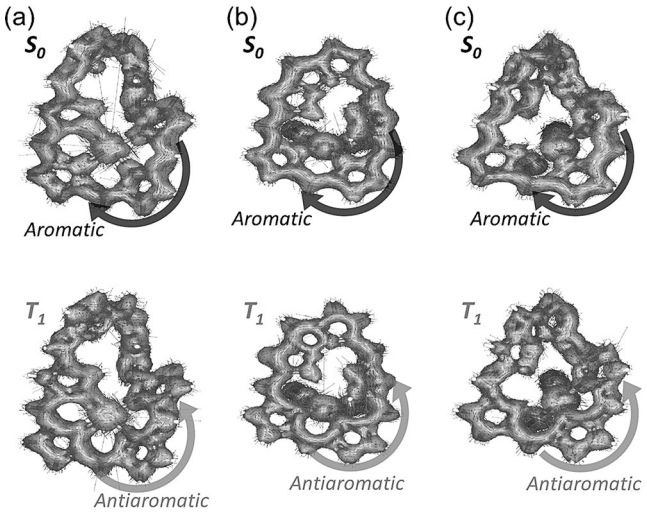

Figure 5. ACID plots of a) Pd28H, b) Rh22P, and c) Rh24P in the ground (top) and triplet (bottom) states. Hydrogen atoms and meso-pentafluorophenyl groups omitted for clarity. For magnified images, see Figures S14–S16.

S_0 state indicate aromaticity whereas counterclockwise ring currents in the T_1 state portray the antiaromatic nature of the compounds. Collectively, these calculated indices for defining the aromaticity are consistent with the optical spectroscopy results, providing evidence for the reversal of aromaticity in the T_1 state ("Baird's rule") in stable Möbius aromatic systems.

In summary, we have extracted the T_1 absorption spectra of Hückel/Möbius aromatic expanded porphyrins by femtosecond time-resolved optical spectroscopy, which enabled a comparative analysis of the optical spectroscopic features of the S_0 and T_1 states. With the help of quantum calculations, in-depth analysis of the absorption spectra of the S_0 and T_1 states revealed that the aromaticity in the S_0 state is reversed to antiaromaticity in the T_1 state in Möbius aromatic systems as well as in Hückel aromatic systems. This study represents the first characterization of excited-state aromaticity in stable Möbius aromatic compounds. The realization of metalated Möbius antiaromatic expanded porphyrins and research on their excited-state aromaticity remain to be challenging.

Acknowledgements

The research at Yonsei University was supported by the Samsung Science and Technology Foundation (SSTF-BA1402-10). The quantum calculations were performed using the supercomputing resources of the Korea Institute of Science and Technology Information (KISTI). The work at Kyoto was supported by the JSPS (KAKENHI Grants 26810021, 25220802, and 25620031). We thank Prof. Rzepa for a copy of the linking-number program.

Keywords: antiaromaticity · aromaticity · Baird's rule · electronic structure · porphyrinoids

How to cite: *Angew. Chem. Int. Ed.* **2016**, *55*, 6487–6491
Angew. Chem. **2016**, *128*, 6597–6601

[1] V. I. Minkin, M. N. Glukhovtsev, B. Y. Simkin, *Aromaticity and Antiaromaticity: Electronic and Structural Aspects*, Wiley, New York, **1994**.
[2] a) P. v. R. Schleyer, *Chem. Rev.* **2005**, *105*, 3433–3435; b) T. M. Krygowski, H. Szatylowicz, O. A. Stasyuk, J. Dominikowska, M. Palusiak, *Chem. Rev.* **2014**, *114*, 6383–6422.
[3] E. Heilbronner, *Tetrahedron Lett.* **1964**, 1923.
[4] a) H. S. Rzepa, *Chem. Rev.* **2005**, *105*, 3697–3715; b) R. Herges, *Chem. Rev.* **2006**, *106*, 4820–4842.
[5] D. Ajami, O. Oeckler, A. Simon, R. Herges, *Nature* **2003**, *426*, 819.
[6] a) M. Stępień, L. Latos-Grażyński, N. Sprutta, P. Chwalisz, L. Szterenberg, *Angew. Chem. Int. Ed.* **2007**, *46*, 7869–7873; *Angew. Chem.* **2007**, *119*, 8015–8019; b) M. Stépień, N. Sprutta, L. Latos-Grazyński, *Angew. Chem. Int. Ed.* **2011**, *50*, 4288–4340; *Angew. Chem.* **2011**, *123*, 4376–4430; c) B. Szyszko, N. Sprutta, P. Chwalisz, M. Stépień, L. Latos-Grazyński, *Chem. Eur. J.* **2014**, *20*, 1985–1997; d) M. Pawlicki, L. Latos-Grazyński, *Chem. Asian J.* **2015**, *10*, 1438–1451.
[7] a) Y. Tanaka, S. Saito, S. Mori, N. Aratani, H. Shinokubo, N. Shinata, Y. Higuchi, Z. S. Yoon, K. S. Kim, S. B. Noh, J. K. Park, D. Kim, A. Osuka, *Angew. Chem. Int. Ed.* **2008**, *47*, 681–684; *Angew. Chem.* **2008**, *120*, 693–696; b) J. Sankar et al., *J. Am. Chem. Soc.* **2008**, *130*, 13568–13579; c) Z. S. Yoon, A. Osuka, D. Kim, *Nat. Chem.* **2009**, *1*, 113–122.
[8] N. C. Baird, *J. Am. Chem. Soc.* **1972**, *94*, 4941–4948.
[9] a) H. Ottosson, *Nat. Chem.* **2012**, *4*, 969–971; b) M. Rosenberg, C. Dahlstrand, K. Kilsa, H. Ottosson, *Chem. Rev.* **2014**, *114*, 5379–5425.
[10] a) J. Zhu, H. A. Fogarty, H. Möllerstedt, M. Brink, H. Ottosson, *Chem. Eur. J.* **2013**, *19*, 10698–10707; b) F. Feixas, J. Vandenbussche, P. Bultinck, E. Matito, M. Sola, *Phys. Chem. Chem. Phys.* **2011**, *13*, 20690–20703; c) B. C. Streifel, J. L. Zafra, G. L. Espejo, C. J. Gómez-García, J. Casado, J. D. Tovar, *Angew. Chem. Int. Ed.* **2015**, *54*, 5888–5893; *Angew. Chem.* **2015**, *127*, 5986–5991; d) R. Papadakis, H. Ottosson, *Chem. Soc. Rev.* **2015**, *44*, 6472–6493; e) R. K. Mohamed, S. Mondal, K. Jorner, T. F.

Delgado, V. V. Lobodin, H. Ottosson, I. V. Alabugin, *J. Am. Chem. Soc.* **2015**, *137*, 15441 – 15450; f) K. Jorner, F. Feixas, R. Ayub, R. Lindh, M. Solà, H. Ottosson, *Chem. Eur. J.* **2016**, *22*, 2793 – 2800.

[11] a) H. J. Wörner, F. Merkt, *Angew. Chem. Int. Ed.* **2006**, *45*, 293 – 296; *Angew. Chem.* **2006**, *118*, 299 – 302; b) H. Ottosson, K. Kilså, K. Chajara, M. C. Piqueras, R. Crespo, H. Kato, D. Muthas, *Chem. Eur. J.* **2007**, *13*, 6998 – 7005; c) H. J. Wörner, F. Merkt, *Angew. Chem. Int. Ed.* **2009**, *48*, 6404 – 6424; *Angew. Chem.* **2009**, *121*, 6524 – 6545.

[12] a) Y. M. Sung, M.-C. Yoon, J. M. Lim, H. Rath, K. Naoda, A. Osuka, D. Kim, *Nat. Chem.* **2015**, *7*, 418 – 422; b) Y. M. Sung, J. Oh, W. Kim, H. Mori, A. Osuka, D. Kim, *J. Am. Chem. Soc.* **2015**, *137*, 11856 – 11859.

[13] a) J. L. Sessler, S. J. Weghorn, V. Lynch, M. R. Johnson, *Angew. Chem. Int. Ed. Engl.* **1994**, *33*, 1509 – 1512; *Angew. Chem.* **1994**, *106*, 1572 – 1575; b) E. Vogel et al., *Angew. Chem. Int. Ed.* **1995**, *34*, 2511 – 2514; *Angew. Chem.* **1995**, *107*, 2705 – 2709; c) M. Bröring, H.-J. Dietrich, J. Dörr, G. Hohlneicher, J. Lex, N. Jux, C. Pütz, M. Roeb, H. Schmickler, E. Vogel, *Angew. Chem. Int. Ed.* **2000**, *39*, 1105 – 1108; *Angew. Chem.* **2000**, *112*, 1147 – 1150.

[14] a) M. Stępień, N. Sprutta, L. Latos-Grażyński, *Angew. Chem. Int. Ed.* **2011**, *50*, 4288 – 4340; *Angew. Chem.* **2011**, *123*, 4376 – 4430; b) S. Saito, A. Osuka, *Angew. Chem. Int. Ed.* **2011**, *50*, 4342; *Angew. Chem.* **2011**, *123*, 4432; c) A. Osuka, S. Saito, *Chem. Commun.* **2011**, *47*, 4330.

[15] a) M.-C. Yoon, S. Cho, M. Suzuki, A. Osuka, D. Kim, *J. Am. Chem. Soc.* **2009**, *131*, 7360 – 7367; b) J.-Y. Shin, M.-C. Yoon, J. M. Lim, Z. S. Yoon, A. Osuka, D. Kim, *Chem. Soc. Rev.* **2010**, *39*, 2751 – 2767; c) S. Cho, Z. S. Yoon, K. S. Kim, M.-C. Yoon, D.-G. Cho, J. L. Sessler, D. Kim, *J. Phys. Chem. Lett.* **2010**, *1*, 895 – 900; d) H. Ottosson, K. E. Borbas, *Nat. Chem.* **2015**, *7*, 373 – 375; e) B. Szyszko, A. Białońska, L. Szterenberg, L. Latos-Grażyński, *Angew. Chem. Int. Ed.* **2015**, *54*, 4932 – 4936; *Angew. Chem.* **2015**, *127*, 5014 – 5018.

[16] S. Mori, S. Soji, R. Taniguchi, A. Osuka, *Inorg. Chem.* **2005**, *44*, 4127 – 4129.

[17] a) S. Mori, J.-Y. Shin, S. Shimizu, F. Ishikawa, H. Furuta, A. Osuka, *Chem. Eur. J.* **2005**, *11*, 2417 – 2425; b) J. K. Park, Z. S. Yoon, M.-C. Yoon, K. S. Kim, S. Mori, J.-Y. Shin, A. Osuka, D. Kim, *J. Am. Chem. Soc.* **2008**, *130*, 1824 – 1825.

[18] a) E. Pacholska-Dudziak, J. Skonieczny, M. Pawlikchi, L. Szterenberg, Z. Ciunik, L. Latos-Grażyński, *J. Am. Chem. Soc.* **2008**, *130*, 6182 – 6195; b) T. Higashino, J. M. Lim, T. Miura, S. Saito, J.-Y. Shin, D. Kim, A. Osuka, *Angew. Chem. Int. Ed.* **2010**, *49*, 4950 – 4954; *Angew. Chem.* **2010**, *122*, 5070 – 5074; c) T. Higashino, B. S. Lee, J. M. Lim, D. Kim, A. Osuka, *Angew. Chem. Int. Ed.* **2012**, *51*, 13105 – 13108; *Angew. Chem.* **2012**, *124*, 13282 – 13285.

[19] M.-C. Yoon, P. Kim, H. Yoo, S. Shimizu, T. Koide, S. Tokuji, S. Saito, A. Osuka, D. Kim, *J. Phys. Chem. B* **2011**, *115*, 14928 – 14937.

[20] M. Gouterman, *J. Mol. Spectrosc.* **1963**, *11*, 108 – 107.

[21] P. v. R. Schleyer, C. Maerker, A. Dransfeld, H. Jiao, N. J. R. v. E. Hommes, *J. Am. Chem. Soc.* **1996**, *118*, 6317 – 6318.

[22] a) S. M. Rappaport, H. S. Rzepa, *J. Am. Chem. Soc.* **2008**, *130*, 7613 – 7619; b) H. S. Rzepa, *Org. Lett.* **2008**, *10*, 949 – 952; c) C. S. Wannere, H. S. Rzepa, B. C. Rinderspacher, A. Paul, C. S. M. Allan, H. F. Schaefer, P. v. R. Schleyer, *J. Phys. Chem. A* **2009**, *113*, 11619 – 11629; d) H. Fliegl, D. Sundholm, F. Pichierri, *Phys. Chem. Chem. Phys.* **2011**, *13*, 20659 – 20665.

[23] a) R. Herges, D. Geuenich, *J. Phys. Chem. A* **2001**, *105*, 3214 – 3220; b) D. Geuenich, K. Hess, F. Köhler, R. Herges, *Chem. Rev.* **2005**, *105*, 3758 – 3772.

Received: February 29, 2016
Revised: March 22, 2016
Published online: April 15, 2016

